Global Change Biology

Global Change Biology (2013) **19**, 1919–1929, doi: 10.1111/gcb.12158

Ocean acidification and warming scenarios increase microbioerosion of coral skeletons

CATALINA REYES-NIVIA*†, GUILLERMO DIAZ-PULIDO‡, DAVID KLINE†, OVE-HOEGH GULDBERG*† and SOPHIE DOVE*†

*Australian Research Council Centre of Excellence for Coral Reef Studies, St. Lucia, Queensland 4072, Australia, †School of Biological Sciences and Global Change Institute, University of Queensland, St. Lucia, Queensland 4072, Australia, ‡Griffith School of Environment and Australian Rivers Institute – Coast & Estuaries, Griffith University, Nathan Campus, Nathan, Queensland 4111, Australia

Abstract

Biological mediation of carbonate dissolution represents a fundamental component of the destructive forces acting on coral reef ecosystems. Whereas ocean acidification can increase dissolution of carbonate substrates, the combined impact of ocean acidification and warming on the microbioerosion of coral skeletons remains unknown. Here, we exposed skeletons of the reef-building corals, *Porites cylindrica* and *Isopora cuneata*, to present-day (Control: 400 μatm – 24 °C) and future pCO_2–temperature scenarios projected for the end of the century (Medium: +230 μatm – +2 °C; High: +610 μatm – +4 °C). Skeletons were also subjected to permanent darkness with initial sodium hypochlorite incubation, and natural light without sodium hypochlorite incubation to isolate the environmental effect of acidic seawater (i.e., $\Omega_{aragonite}$ <1) from the biological effect of photosynthetic microborers. Our results indicated that skeletal dissolution is predominantly driven by photosynthetic microborers, as samples held in the dark did not decalcify. In contrast, dissolution of skeletons exposed to light increased under elevated pCO_2–temperature scenarios, with *P. cylindrica* experiencing higher dissolution rates per month (89%) than *I. cuneata* (46%) in the high treatment relative to control. The effects of future pCO_2–temperature scenarios on the structure of endolithic communities were only identified in *P. cylindrica* and were mostly associated with a higher abundance of the green algae *Ostreobium* spp. Enhanced skeletal dissolution was also associated with increased endolithic biomass and respiration under elevated pCO_2–temperature scenarios. Our results suggest that future projections of ocean acidification and warming will lead to increased rates of microbioerosion. However, the magnitude of bioerosion responses may depend on the structural properties of coral skeletons, with a range of implications for reef carbonate losses under warmer and more acidic oceans.

Keywords: coral skeleton, dissolution, endolithic algae, *Isopora*, microbioerosion, ocean acidification and warming, *Ostreobium*, *Porites*

Received 17 June 2012; revised version received 21 January 2013 and accepted 22 January 2013

Introduction

Due to the natural equilibrium between gases in the atmosphere and ocean, increased atmospheric pCO_2 from anthropogenic sources is absorbed by the ocean surface, decreasing seawater pH, and causing ocean acidification (Kleypas *et al.*, 2001; Caldeira & Wickett, 2003). This change depletes the concentration of carbonate ions (CO_3^{2-}), lowering the saturation state (Ω) of the mineral phases of calcium carbonate (Orr *et al.*, 2005), and reducing the accretion potential of coral reef ecosystems (Kleypas *et al.*, 2001; Hoegh-Guldberg *et al.*, 2007). The increase in atmospheric pCO_2 and other greenhouse gases has also caused an increase in the sea surface temperature by 0.4–1.0 °C in the past four decades (Kleypas *et al.*, 2008). Whereas increasing temperatures in shallow waters may counteract the effect of ocean acidification on carbonate saturation states (Andersson *et al.*, 2008), thermal stress due to ocean warming can detrimentally affect the health of reef organisms, potentially contributing to coral reef degradation (Hughes *et al.*, 2003; Hoegh-Guldberg *et al.*, 2007).

Projected increases in seawater (SW) acidity and temperature in the coming decades (Ipcc, 2007) are expected to reduce calcification (Langdon & Atkinson, 2005; Jokiel *et al.*, 2008) and increase dissolution (Anthony *et al.*, 2008; Andersson *et al.*, 2009; Diaz-Pulido *et al.*, 2012) of corals and crustose coralline algae (CCA). These changes are likely to further increase bioerosion rates of reef carbonates (Manzello *et al.*, 2008; Wisshak *et al.*, 2012), potentially disrupting the balance between carbonate accumulation and erosion. Tribollet *et al.* (2009) demonstrated that increased SW pCO_2 enhanced

Correspondence: Catalina Reyes-Nivia, School of Biological Sciences and Global Change Institute, University of Queensland, St. Lucia, Queensland 4072, Australia, tel. +61 7 3365 3548, fax +61 7 3365 2665, e-mail: catalina.reyes@uq.edu.au

dissolution rates of coral carbonates, yet the relative contributions of different bioerosion processes and how they may be altered by the combined effect of ocean acidification and warming are still poorly understood (Atkinson & Cuet, 2008; Andersson & Gledhill, 2012).

The most important microborers of carbonate skeletons are endolithic green and red algae, cyanobacteria, and fungi (Golubic *et al.*, 1981; Le Campion-Alsumard *et al.*, 1995). Among these organisms, the green alga *Ostreobium* sp. is associated with high rates of bioerosion (Le Campion-Alsumard *et al.*, 1995; Tribollet, 2008b). Microbioerosion is most likely caused by chemical dissolution driven by the metabolic activity of internal microborers (Garcia-Pichel, 2006). While recent evidence indicates that the dissolution of *Porites* sp. skeletons increases under elevated pCO_2 conditions (Tribollet *et al.*, 2009), little is known about the combined effect of future ocean acidification and warming projections on the microbioerosion of different substrates. Although the increased dissolution of CCA under elevated pCO_2 and temperature conditions has been linked to the presence of microborers, such a link has not been empirically quantified (Martin & Gattuso, 2009; Diaz-Pulido *et al.*, 2012).

In this study we tested the hypothesis that combined ocean acidification and warming would alter microbioerosion processes on coral skeletons. We did not investigate the individual effect of increased SW pCO_2 and temperature, or the relative contribution of each process on carbonate bioerosion. Rather, we addressed the question of how microbioerosion may respond to future emission scenarios by the Intergovernmental Panel of Climate Change (IPCC), as increases in atmospheric pCO_2 concurrently lead to both ocean acidification and warming (Meehl *et al.*, 2007). Comparing present-day conditions with two elevated pCO_2–temperature scenarios, we explored how skeletons of *Porites cylindrica* (branching growth form) and *Isopora cuneata* (encrusting growth form) respond to biochemically mediated dissolution. The biological effect of photosynthetic microborers on skeletal dissolution was isolated from the environmental effect of elevated SW pCO_2–temperature (i.e., dissolution if $\Omega < 1$ as this variable is sensitive to both pCO_2 and temperature). Also, the effects of experimental pCO_2–temperature scenarios on biological and ecological responses of endolithic algae were quantified.

Materials and methods

General protocol and CO_2–temperature system

The experiment was conducted during austral spring from September to November 2010, at Heron Island Research Station, southern Great Barrier Reef (GBR; 23°26′S, 151°54′E). Coral skeletons were exposed to three SW pCO_2–temperature scenarios, offset from seasonally relevant and fluctuating reef conditions: 1 – Control (+0 μatm – +0 °C); 2 – Medium (+230 μatm – +2 °C); 3 – High (+610 μatm – +4 °C). Offsets for medium and high treatments were based on IPCC scenarios, representing 'reduced' (B2) and 'business as usual' (A1FI) fossil fuel use (Ipcc, 2007).

A pCO_2–temperature controlled system was used to treat filtered SW (10 μm) in three large sealed reservoirs (10 kL) before entering the experimental tanks. Acidification of SW was achieved by bubbling a fine curtain of CO_2 enriched and CO_2 depleted air through each reservoir. The CO_2–depleted air was produced by passing compressed air through two desiccant columns (Model 106-C, W. A. Hammond Drierite, Australia) filled with soda lime. The CO_2 dose was determined by a pCO_2 analyzer and controlled by a custom-built software package (CO_2-Pro™, Pro-Oceanus Systems Inc. Canada). Temperature was controlled by three industrial heater-chillers (HWP017-1BB, Accent Air, Australia). The system allowed SW pCO_2 and temperature to follow seasonally appropriate fluctuations measured at a reference field site (Harry's Bommie, Heron Island, GBR). Field data were continuously recorded by a MAPCO$_2$ system to monitor ocean acidification (PMEL Carbon Program, NOAA and CSIRO, Australia http://www.pmel.noaa.gov/co2/story/Heron+Island). The reference averages for SW pCO_2 and temperature were 381 μatm ($\pm$ 4.4 SEM) and 24 °C ($\pm$ 0.1 SEM), providing a near perfect match to the control conditions (see Table 1). Seawater samples for total alkalinity (A_T) analysis were taken at noon and midnight at the end of the study to include the periods when the SW alkalinity and pH are likely to be most divergent. Seawater samples were analyzed by potentiometric titration (T50 Titrator, Mettler Toledo, Switzerland) and calibrated using a Dickson standard, with alkalinity replicates within a sample having a maximum error of 3 μmol kg^{-1} (Dickson *et al.*, 2003). The carbonate chemistry of SW was calculated using CO2SYS (Pierrot *et al.*, 2006) with temperature, pCO_2, A_T, and salinity (35.8 $\pm$ 0.2 SEM; $n = 10$) as the input parameters, and pH SW scale (kg mol^{-1}), aragonite saturation state (Ω_{arag}), bicarbonate (HCO_3^-), and carbonate (CO_3^{2-}) as output parameters. Constants were obtained from Mehrbach *et al.* (1973) and modified by Dickson & Millero (1987).

Sample collection and preparation

Samples of *Porites cylindrica* and *Isopora cuneata* were collected from the reef flat and shallow reef crest of Heron Island and Wistari Reef, respectively. Samples were cut using a diamond saw to obtain 125 experimental substrates of each coral (*I. cuneata* ca. 3 × 3 cm and *P. cylindrica* ca. 6 cm long and 3 cm in diameter). These two common reef-building corals harbor high abundances of endolithic algae (Fig. S1). Coral tissue was removed from the skeletons by airbrushing to simulate recently dead coral substrates while retaining their complement of endolithic algae (Fine *et al.*, 2005). By removing the coral tissue, endolithic microborers were subjected to light environments that mimic natural light intensities (Fine & Loya, 2002) following coral mortality after mass bleaching events, air exposure at low tide, or corallivory (Baird & Marshall, 2002; Reyes-Nivia *et al.*, 2004; Hoegh-Guldberg *et al.*, 2005).

Table 1 Summary of mean seawater temperature and pCO_2 concentration determined for the 8 weeks experimental period, along with carbonate parameters estimated for three distinct pCO_2–temperature scenarios at the end of the experiment. Temperature and pCO_2 are mean values (± SEM) recorded at <30 min intervals over the length of the experiment. Input temperature (T), seawater pCO_2, and total alkalinity (A_T) are means (± SEM) of 10 seawater replicates collected at the end of the study. Output pH (seawater scale kg mol^{-1}), aragonite saturation state (Ω_{arag}), bicarbonate (HCO_3^-), and carbonate (CO_3^{2-}) were estimated using the program CO2SYS (Pierrot *et al*., 2006).

	pCO_2–temperature conditions		Seawater carbonate chemistry						
	8 weeks mean		Input parameters			Output parameters			
Scenarios	T (°C)	pCO_2 (μatm)	T (°C)	pCO_2 (μatm)	A_T (μmol kg^{-1})	pH	Ω_{arag}	HCO_3^- (μmol kg^{-1})	CO_3^{2-} (μmol kg^{-1})
Control	24.0 ± 0.0	401 ± 0.8	23.4 ± 0.1	391 ± 2.2	2239 ± 2.7	8.03 ± 0.002	3.1 ± 0.02	1747 ± 1.7	199 ± 1.4
Medium	26.0 ± 0.1	639 ± 1.3	25.6 ± 0.1	651 ± 8.0	2240 ± 2.4	7.84 ± 0.005	2.4 ± 0.02	1870 ± 3.3	150 ± 1.3
High	28.0 ± 0.1	1012 ± 1.7	29.2 ± 0.1	1103 ± 29.9	2239 ± 2.6	7.65 ± 0.011	1.8 ± 0.04	1960 ± 6.3	114 ± 2.5

Experimental design

Each pCO_2–temperature treatment had five replicate tanks (15 l plastic aquaria), which received SW from the reservoirs at a constant flow rate (1 l min^{-1}). Small pumps were placed in each aquarium to ensure water circulation. Each tank contained seven experimental subsamples of each type of skeleton (where type is defined by coral source). Samples were randomized among tanks and treatments to account for variability in the initial biomass of endolithic algae. Epilithic algae were removed every 48 h from the samples using a soft toothbrush to reduce potential confounding effects caused by turf growth response and resultant shading under different conditions. Neutral density filters (LEE filter 0.3) covered each tank to reduce light exposure by 51% without affecting the color balance of incoming light. Light was measured in the tanks at 10 cm depth, using a LI-192 Underwater Quantum Sensor (Li-COR), with midday levels ranging from 600 to 1200 μmol quanta m^{-2} s^{-1} depending on cloud cover.

To quantify the environmental effect of SW $pCO2$–temperature conditions on skeletal dissolution, four additional tanks per treatment were maintained constantly in the dark following an initial 10 h sample soak in a 10% sodium hypochlorite solution. This solution was only used on the dark samples to eliminate all microborers, detected as a loss of pigmentation, at the start of the experiment and thereby provide an abiotic skeleton. For these samples, the reestablishment of photosynthetic microborers was inhibited by the perpetual maintenance in the dark. This procedure, however, could not guarantee the prevention of the resettlement of heterotrophic microbes over the experimental process. Dark samples were also cleaned every 48 h with a soft toothbrush during the experimental period. Each dark tank contained five samples of each type of skeleton.

Response variables

To estimate negative or positive change in $CaCO_3$ of the coral skeletons, a high-precision buoyant weight method was used (Davies, 1989). Microbioerosion (also referred to as biological dissolution) and/or calcification were calculated as the per cent change in buoyant weight of skeletons between the end (day 60) and beginning (day 0) of the experiment. Monthly rates of microbioerosion were expressed as changes in buoyant weight normalized to total surface area (mg cm^{-2} $month^{-1}$), which was determined using a modified wax dipping method (Holmes, 2008). Changes in buoyant weight were further converted into rates of dissolved $CaCO_3$ normalized to area (mg cm^{-2} $month^{-1}$) using a SW density of 1.024 g cm^{-3} and coral skeletons microdensity of 2.46 g cm^{-3} (± 0.05 SEM, n = 15) for *P. cylindrica* and 2.69 g cm^{-3} (± 0.01 SEM, n = 15) for *I. cuneata*. Microdensity was determined by applying the skeleton density method (Davies, 1989).

To estimate the biomass of endolithic algae in coral skeletons, the loss on ignition (LOI) method (Heiri *et al*., 2001) was applied. Biomass was calculated as milligrams of endolithic algae normalized to surface area (mg cm^{-2}). A subset of 45 samples per type of skeleton was used to quantify the biomass at the end of the study period. Samples were thoroughly cleaned under a dissecting microscope to ensure only endolithic organisms were preserved (Fig. S1). Skeletons were dried at 60 °C until they reached constant weight and then combusted at 550 °C for 4 h to oxidize all organic matter (Heiri *et al*., 2001; Cuif *et al*., 2004). Samples were weighed before and after combustion using a high-precision balance. Weight loss after combustion was corrected for each sample to account for the organic compounds within coral skeletons (Cuif *et al*., 1999). A 1% correction factor was used as thermogravimetric analysis (from 20 to 550 °C) showed a total organic content (intracrystalline) of 1–1.2% for six skeletons of different coral species (Cuif *et al*., 2004).

To identify the ecological responses of the endolithic community, the composition and relative abundance of microborers were examined by the method of Diaz-Pulido & Mccook (2002) with the following modifications: Surfaces colonized by endolithic algae were transversally cut using a diamond saw to obtain standardized areas of ca. 0.5 × 0.5 cm; and estimates of the relative abundance of endolithic taxa were determined by the percent cover in 6 microscopic fields per slide at 40× magnification. Species were identified based on the literature

available (Lukas, 1974; Humm & Wicks, 1980; Le Campion-Alsumard *et al*., 1995; Nagarkar, 1998; Tribollet, 2008b) and prior to the recent identification of cryptic diversity within the genus *Ostreobium* (Gutner-Hoch & Fine, 2011). A total of 10 slides per treatment from each skeleton were used for identification and abundance estimations.

The rate of dark respiration of the endolithic communities was measured and related to patterns of microbioerosion. Respirometry assays were conducted for 15 min at 0 μmol quanta m^{-2} s^{-1} following at least 6 h of dark acclimation. Respiration estimates were conducted on the same subset of samples used for biomass quantification. Measurements were carried out using eight recirculating respirometry chambers (140 cm^3) following a similar protocol to Crawley *et al.* (2010). Oxygen fluxes for each sample were normalized to biomass of endolithic algae (μmol O_2 h^{-1} mg^{-1}).

To explore the variability in pH between interstitial and bulk SW, pH profiles within *P. cylindrica* skeletons were conducted using fast-responding pH microsensors and a lab-based system (pH-500 microsensor, 4-channel Multimeter, SensorTrace software, Unisense, Denmark). Holes of 5 mm depth were drilled (3 weeks before profiling) on the skeleton surface with a 0.5 mm diameter drill bit. A reference electrode and the pH microsensor (500 μm tip diameter) were connected to a microsensor amplifier coupled to a computer. Calibration was linearly performed using three NIST-certified pH buffers (Mettler Toledo, Switzerland). Depth profiles of pH were done under dark and light conditions (900 quanta m^{-2} s^{-1}; Ocean light, Aqua Medic, Germany) using a manual micromanipulator. Measurements were conducted under control pCO_2–temperature conditions at the end of the study.

Data analysis

Two-way nested ANOVAs, using a least-square mean, were applied to test whether microbioerosion, calcification, and biomass varied among pCO_2–temperature scenarios and types of skeleton. pCO_2–temperature scenario and type of skeleton were treated as fixed factors, tanks as random replicates nested within the pCO_2–temperature x type of skeleton interaction, and samples were nested within tanks. If a significant interaction between treatment and type of skeleton was found, a one-way nested ANOVA was used to test the fixed effect of pCO_2–temperature scenario on the dependent variables for each type of skeleton. Tanks were again treated as nested replicates with samples being nested within tanks. When no effect of tanks was identified ($P > 0.25$) tanks were pooled in a one-way ANOVA using samples as replicates (Underwood, 1997). *Post hoc* pairwise analyses were applied using Tukey's tests. The percentage of microbioerosion/calcification was arcsine transformed whereas biomass was log transformed. ANOVA's assumptions of variance homogeneity and normality were tested using Levene's and K-S, respectively (Sokal & Rohlf, 1995). Analyses were done using STATISTICA 10.

Multivariate analyses were applied to examine differences in community structure of endolithic algae among pCO_2–temperature scenarios. The percentage of relative abundance was arcsine transformed. The Bray–Curtis similarity measure was used to produce a resemblance matrix (Clarke, 1993; Anderson *et al*., 2008). A one-way nested PERMANOVA was applied with pCO_2–temperature scenario as a fixed factor and tanks as replicates. Samples were nested within tanks. As no tank effects were identified in *P. cylindrica* skeletons, tanks were pooled to perform a one-way PERMANOVA. Values of the pseudo-F statistic were computed using 9999 permutations, and pairwise comparisons were then applied. Ordination by principal coordinates analysis (PCO) was used to spatially visualize dissimilarities in endolithic community structure among pCO_2–temperature scenarios. Potential indicator species or species assemblages characterizing the observed groups were determined by Spearman correlations (vector lengths >0.5) and then superimposed on the ordination space. Analyses were done using PERMANOVA+ for PRIMER v6. To further explore the effects of pCO_2–temperature scenarios on the relative abundance of dominant endolithic species, a one-way ANOVA was used on selected taxa.

Regression analyses with all data and by individual treatments were applied using a least-square approach to explore the relationship between microbioerosion and: (i) biomass of endolithic algae, (ii) dark respiration rates per unit biomass, and (iii) relative abundance of *Ostreobium* spp. Data were checked for leverage points to avoid large effects on regression coefficients.

Results

Changes in skeletal weight

All coral skeletons harboring endolithic algae (under natural day–night cycles and not pretreated with sodium hypochlorite) lost $CaCO_3$ (Fig. 1a). Total microbioerosion (% reduction over 2 months) of both *I. cuneata* and *P. cylindrica* skeletons increased under the two elevated pCO_2–temperature scenarios (Fig. 1a, Table 2), and the type of skeleton and scenario had a significant effect on microbioerosion responses (Table 2). Carbonate microbioerosion on *I. cuneata* substrates significantly increased in the medium relative to control treatment, but showed no further increase in the high pCO_2 –temperature treatment (Table 2). Microbioerosion on *P. cylindrica* steadily increased from control to high pCO_2–temperature scenario (Table 2). High variability in the microbioerosion of both types of coral skeletons was observed between tanks under the same pCO_2–temperature scenario (Table 2).

Skeletons without photosynthetic endolithic algae (under full dark conditions and pretreated with sodium hypochlorite) showed no signs of $CaCO_3$ dissolution, with a positive increase in buoyant weight observed at the end of the experiment. Net calcification (% increase over 2 months) was similar between experimental substrates and pCO_2–temperature scenarios (Fig. 1a, Table 2). Again, high variability in the calcification response of both *I. cuneata* and *P. cylindrica* was observed between tanks within the same pCO_2–temperature scenario (Table 2).

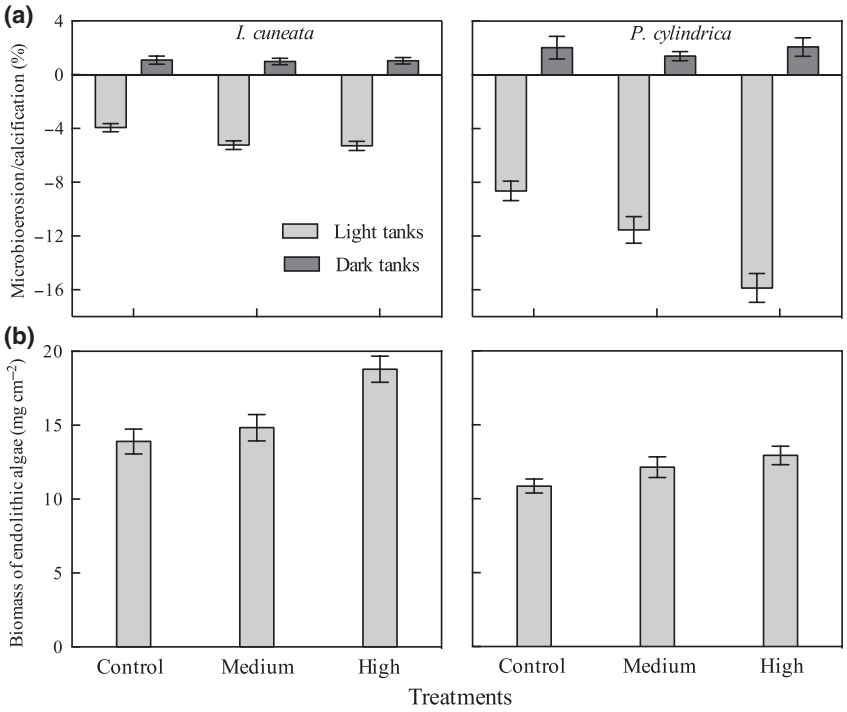

Fig. 1 Effects of pCO_2–temperature scenarios on (a) microbioerosion/calcification (%) and (b) biomass of endolithic algae (mg cm^{-2}) in skeletons of *Isopora cuneata* and *Porites cylindrica*. Data correspond to means ± SEM. Calcification data correspond to skeletons exposed to full dark conditions (n = 20 samples for each treatment). Microbioerosion data correspond to samples under natural light (n = 25 samples for each treatment) as well as biomass of endolithic algae (n = 15 samples for each treatment). pCO_2–temperature treatments correspond to present-day conditions (Control: ca. 400 μatm – 24 °C) and two IPCC projected scenarios (Medium/B2: +230 μatm – +2 °C and High/A1FI: +610 μatm – + 4 °C).

Rates of net dissolution by microborers

The rate of skeletal microbioerosion (mg cm^{-2} $month^{-1}$ ± SEM; n = 25 samples per treatment) in *I. cuneata* increased from control (8.04 ± 0.71) to medium (10.65 ± 0.85) and high pCO_2–temperature scenarios (11.76 ± 0.99). *P. cylindrica* exhibited even higher rates of microbioerosion, with a twofold increase from the control to high treatment (control = 12.67 ± 1.26; medium = 17.21 ± 1.44; high = 23.96 ± 2.12). Net dissolution of *I. cuneata* (mg $CaCO_3$ cm^{-2} $month^{-1}$ ± SEM) increased from 32 to 46% under both elevated pCO_2–temperature scenarios relative to the control (control = 12.98 ± 1.15; medium = 17.20 ± 1.37; high =18.99± 1.60), whereas dissolution of *P. cylindrica* increased 89% in the highest scenario (control = 21. 70 ± 2.15; medium= 29.49 ± 2.46; high = 41.05 ± 3.63).

Biomass of endolithic algae

The biomass of endolithic algae (mg cm^{-2}) significantly increased in the high pCO_2–temperature treatment relative to control and medium treatments (Fig. 1b, Table 2). The type of skeleton also influenced the biomass of endolithic algae (Table 2), with significantly higher biomass in *I. cuneata* compared with *P. cylindrica* substrates (Fig. 1b).

Community structure of endolithic algae

The filamentous algae *Ostreobium* spp. (*O. quekettii* and *O. constrictum*) and the cyanobacterium *Plectonema terebrans* accounted for 65–90% of the total abundance across the treatments (Fig. 2). Less abundant species included two cyanobacteria (*Hyella* sp., and *Mastigocoleus testarum*), two unidentified coccoid species, and three epilithic cyanobacteria (*Oscillatoria* spp., *Spirulina* sp., and an unidentified encapsulated-like species labeled as Morpho1; Fig. 2). Fungi were rare from the endolithic communities and were included in the category 'Other' (Fig. 2).

The endolithic community structure in *P. cylindrica* skeletons significantly varied among pCO_2–temperature scenarios (PERMANOVA: $F_{2,25}$ = 4.381; P < 0.0001; Fig. 2). Pair-wise comparisons revealed differences among all treatments. The first two axes of PCO analysis explained 67% of the variance in endolithic algae distribution. *Hyella* sp., Coccoid1, and Morpho1 were

Table 2 Two-way nested ANOVA testing the effects of pCO_2–temperature scenarios and coral skeletons (*Isopora cuneata* and *Porites cylindrica*) on microbioerosion, calcification, and biomass of endolithic algae. A one-way ANOVA was also applied to test the effect of pCO_2–temperature scenarios on microbioerosion for each coral skeleton. Control pCO_2–temperature = C; Medium pCO_2–temperature = M; High pCO_2–temperature = H; *I. cuneata* = IC; *P. cylindrica* = PC.

Source of variation	df	MS	F	*P*	Post hoc Tukey
Microbioerosion					
Scenario	2	213.5	12.7	<0.001	
Skeleton	1	1964.5	117.3	<0.001	
Scenario × Skeleton	2	66.94	3.9	0.031	
Tank (Scenario × Skeleton)	24	16.77	1.6	0.037	
Error	118	10.01			
I. cuneata					
Scenario	2	30.17	6.26	0.003	M > C; H > C
Error	70	4.81			
P. cylindrica					
Scenario	2	257.60	14.87	<0.001	H > M > C
Error	72	17.31			
Calcification					
Scenario	2	2.7	0.03	0.962	
Skeleton	1	40.0	0.56	0.462	
Scenario × Skeleton	2	2.9	0.04	0.960	
Tank (Scenario × Skeleton)	18	72.4	14.99	<0.001	
Error	88	4.8			
Biomass					
Scenario	2	0.08	8.11	0.002	H > C; H > M
Skeleton	1	0.32	30.76	<0.001	IC > PC
Scenario × Skeleton	2	0.00	0.80	0.462	
Tank (Scenario × Skeleton)	24	0.01	1.64	0.062	
Error	58	0.00			

more abundant under control conditions (PCO1; Fig. 3). *Ostreobium* spp. was dominant in most high pCO_2–temperature treatments and in few medium samples (PCO2; Fig. 3), and significantly increased in the high pCO_2–temperature treatment relative to control (ANOVA: $F_{2,29} = 3.498$; $P < 0.05$; Fig. 2). In contrast, the structure of the endolithic algal community of *I. cuneata* skeletons was not significantly different among pCO_2–temperature scenarios (PERMANOVA: $F_{2,15} = 1.684$; $P = 0.15$). However, the dominance of *P. terebrans* in *I. cuneata* skeletons significantly increased under the two elevated pCO_2–temperature scenarios (ANOVA: $F_{2,29} = 6.375$; $P < 0.05$). The first two axes of PCO analysis explained about 87% of the variance in endolithic algae distribution. Although two main assemblages could be distinguished, the distribution pattern showed high variability among *I. cuneata* samples within a treatment (Fig. 3).

Explanatory variables

Rates of microbioerosion (mg cm^{-2} $month^{-1}$) were related to the biomass of endolithic algae (mg cm^{-2}) for both substrates (*I. cuneata* $R^2 = 0.3094$, $P < 0.001$ and *P. cylindrica* $R^2 = 0.3560$, $P < 0.0001$; Fig. 4). Individual regressions showed similar relationships for the medium and high pCO_2–temperature scenarios (*I. cuneata* $R^2 = 0.4009$, $P < 0.05$ and $R^2 = 0.3219$, $P < 0.05$, respectively; *P. cylindrica* $R^2 = 0.2904$, $P < 0.05$ and $R^2 = 0.4790$, $P < 0.05$, respectively). Rates of microbioerosion were also proportionally related to the rates of dark respiration (μmol O_2 h^{-1} mg^{-1}) for *P. cylindrica* ($R^2 = 0.2529$, $P < 0.001$; Fig. 4), particularly in the medium treatment ($R^2 = 0.6528$, $P < 0.001$). Profiles of pH within this coral skeleton revealed decreases in pH (7.8–7.3 with increasing depth into the skeleton) relative to the control bulk water (8.1) during dark respiration (Fig. 5). The percentage of microbioerosion was also related to the relative abundance of *Ostreobium* spp. for *P. cylindrica* ($R^2 = 0.3869$, $P < 0.05$).

Discussion

Changes in skeletal weight

Here, we demonstrated that dissolution of coral skeletons, driven predominantly by photosynthetic microborers, increased under combined ocean acidification

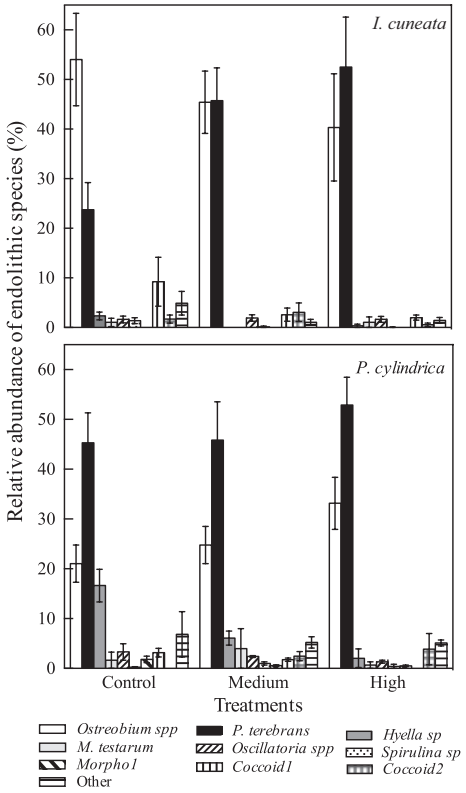

Fig. 2 Relative abundance (%) of endolithic algae and epilithic cyanobacteria that inhabited recently dead coral skeletons of *Isopora cuneata* and *Porites cylindrica* following an 8 weeks colonization period under three CO_2–temperature scenarios. Data correspond to means ± SEM (n = 10 slides per treatment). pCO_2–temperature treatments correspond to present-day conditions (Control: ca. 400 μatm – 24 °C) and two IPCC projected scenarios (Medium/B2: +230 μatm – +2 °C and High/A1FI: +610 μatm – +4 °C).

and warming scenarios. Furthermore, dissolution varied with the pCO_2–temperature scenario and the identity of the coral substrate. This study therefore extends the finding of Tribollet *et al.* (2009) where higher dissolution rates for the skeletons of *Porites lobata* were observed under ocean acidification. In our experiment, skeletons of *P. cylindrica* were more susceptible to biologically mediated dissolution than the skeletons of *I. cuneata*, at least when acidification and warming are combined. This suggests that the skeletal structure of corals (e.g., microskeletal architecture, porosity, density, mineralogy) plays an important role in determining the magnitude of the effects of pCO_2–temperature scenarios on carbonate dissolution. Our interpretation is supported by other studies that demonstrate how the microarchitecture of a range of experimental substrates (e.g., coral, calcite crystals, and mollusk shells) exerts a significant control on the boring abilities of endolithic microborers (Golubic *et al.*, 1975; Kiene *et al.*, 1995; Perry, 1998). As coral carbonates are dominant in most coral reefs and particularly susceptible to microbioerosion (Le Campion-Alsumard *et al.*, 1995; Perry, 1998; Tribollet, 2008a), increased dissolution of coral skeletons under elevated pCO_2–temperature scenarios may alter bioerosional processes, potentially disrupting the carbonate balance in coral reef ecosystems.

The comparison of experimental substrates exposed to dark vs. light conditions suggests that the processes driving dissolution of coral skeletons are predominantly mediated by endolithic algae and not by the saturation state of seawater with respect to aragonite (Ω_{arag}) applied in this study. Skeletons exposed to full dark (i.e., without endolithic algae) and elevated pCO_2–temperature scenarios gained weight, indicating that the lowered Ω_{arag} of bulk SW in our study did not contribute to the dissolution of calcium carbonate. Microbial mediation of carbonate precipitation has been previously observed in carbonate sediments (Dupraz *et al.*, 2009) and this may explain the skeletal calcification under dark conditions. A number of bacterially driven processes (e.g., ammonification, denitrification, and sulfate reduction) may result in increased alkalinity and hypersaturation of Ω inside the coral skeletons, potentially promoting carbonate precipitation (Riding, 2000; Nothdurft *et al.*, 2007). However, understanding the mechanism by which calcification occurred under dark conditions is beyond the scope of this study. Our results therefore suggest that the dissolution of coral skeletons was predominantly mediated by the responses of photosynthetic microborers under a range of pCO_2–temperature scenarios.

The role of endolithic microborers in dissolution processes

Projected ocean acidification and warming scenarios appear to favor biomass accumulation by endolithic algae. Previous studies have also demonstrated increased growth of these organisms under elevated pCO_2 and/or temperature conditions (Fine & Loya, 2002; Tribollet *et al.*, 2009; Diaz-Pulido *et al.*, 2012). Importantly, we found that increased biomass of microborers partially explained the enhanced dissolution rates of coral skeletons under elevated pCO_2–temperature scenarios. A similar relationship was observed for the dissolution of coralline algae under the interaction of high pCO_2 and temperature levels (Diaz-Pulido *et al.*, 2012). Growing evidence suggests that projected acidification and warming scenarios stimulate the biomass of microborers, which in turn increases the dissolution of reef carbonate substrates. Corals and coralline algae are common substrates for endolithic microborers (sensu Golubic *et al.*, 1981). Both are major reef calcifiers and are predicted to experience high mortality under ocean

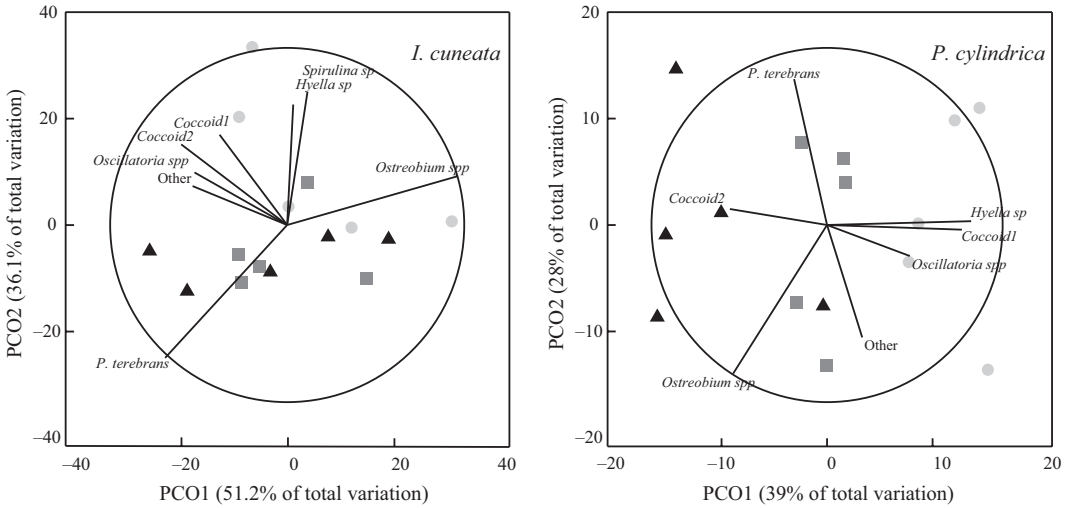

Fig. 3 Principal coordinates ordination (PCO) of the response of endolithic community to three pCO_2–temperature scenarios (Control = circles; Medium = squares; High = triangles) in coral skeletons of *Isopora cuneata* and *Porites cylindrica*. pCO_2–temperature treatments correspond to present-day conditions (Control: ca. 400 μatm – 24 °C) and two IPCC projected scenarios (Medium/B2 scenario: +230 μatm – +2 °C and High/A1FI: +610 μatm – +4 °C). High percentages of the explained variance by the two PCO axes indicate good two-dimensional ordination. Spearman correlation coefficients for the taxa that best correlated (only R > 0.5 is shown) with the two axes are shown as vector overlays (circle indicating a radius of 1).

acidification and/or warming (Baird & Marshall, 2002; Anthony *et al*., 2008; Diaz-Pulido *et al*., 2012). Therefore, an increase in the biomass of endolithic algae is likely to lead to significant bioerosion within coral reef frameworks.

Dark respiration by endolithic algae appears to be another important factor associated with the microbioerosion of the experimental coral skeletons. Decreases in interstitial Ω_{arag} due to the metabolic activity of microbes and boring endoliths may create corrosive conditions that cause skeletal dissolution especially at night (Walter *et al*., 1993; Andersson *et al*., 2007; Tribollet, 2008b). In support of this, we observed significant decreases in the interstitial pH under control conditions, particularly in the dark, with increasing depth into the coral skeleton (e.g., interstitial pH = 7.3 vs. bulk water pH = 8.1; see Fig. 5). Although more replication is certainly required, the obtained data suggest that even more significant decreases in pH may be achieved when the skeletons are surrounded by further acidified bulk seawater (Kleypas *et al*., 2006; Andersson & Gledhill, 2012). More importantly, the potential for reducing the pH below 7.3 could be greatly enhanced under elevated pCO_2–temperature scenarios by the observed increases in both endolithic biomass and dark respiration normalized to biomass. These compounding factors along with the persistent dissolution ability of microborers via acid-generating metabolism (i.e., dark dependent) and Ca^{2+} uptake (i.e., light dependent) (Garcia-Pichel *et al*., 2010; Ramirez-Reinat & Garcia-Pichel, 2012), suggest a widespread increase in the dissolution rates of reef carbonates under elevated pCO_2–temperature scenarios.

It is not totally clear how changes in the structure of the endolithic community may explain the dissolution responses of reef carbonate substrates. However, changes in the abundance of the filamentous algae *Ostreobium* spp., rather than cyanobacteria, appeared to influence the dissolution of particular coral skeletons under elevated pCO_2–temperature scenarios. Other studies have similarly recognized that *Ostreobium* sp. is responsible for most of the dissolution of coral substrates under natural and acidified conditions (Chazottes *et al*., 2002; Tribollet, 2008b; Tribollet *et al*., 2009). This alga is the most common endolithic microborer, inhabiting about 85% of coral species over a wide geographic range (Lukas, 1974; Vogel *et al*., 2000; Försterra & Häeussermann, 2008). Its extraordinary ability to cope with low-light environments (Le Campion-Alsumard *et al*., 1995; Magnusson *et al*., 2007) allows *Ostreobium* spp. to penetrate deeper into carbonate substrates (Tribollet, 2008b; Tribollet *et al*., 2009) and dominate reef environments from 1 to 275 m depth (Kiene *et al*., 1995; Chazottes *et al*., 2009). Given these physiological traits and the enhanced abundance of *Ostreobium* spp. under elevated pCO_2–temperature scenarios, we suggest this alga could accelerate dissolution of carbonates in a wide range of reef environments. Experimental studies simulating climate change scenarios and different light conditions are needed to

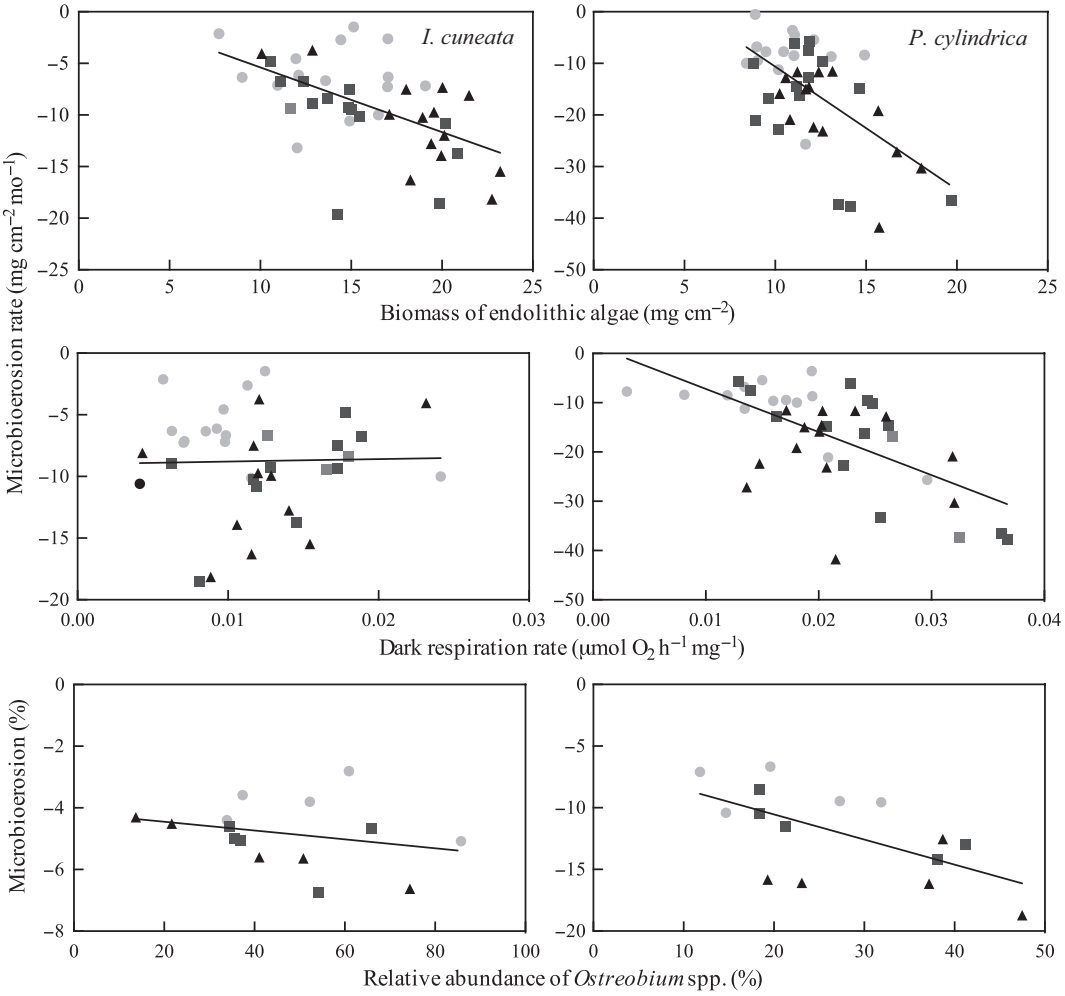

Fig. 4 Relationship between microbioerosion of *Isopora cuneata* and *Porites cylindrica* skeletons and different variables of the endolithic algae. Both types of skeleton were exposed to three pCO_2–temperature scenarios (Control = circles; Medium = squares; High = triangles). The complete data set is plotted and represented by the solid line. Rates of microbioerosion (mg cm^{-2} month^{-1}) vs. biomass of endolithic algae (mg cm^{-2}) for *I. cuneata* ($R^2 = 0.3094$, $P < 0.001$) and *P. cylindrica* ($R^2 = 0.3560$, $P < 0.0001$). Regressions by treatment were significant in the medium and high scenarios for *I. cuneata* ($R^2 = 0.4009$, $P < 0.05$ and $R^2 = 0.3219$, $P < 0.05$) and for *P. cylindrica* ($R^2 = 0.2904$, $P < 0.05$ and $R^2 = 0.4790$, $P < 0.01$, respectively). Rates of microbioerosion (mg cm^{-2} month^{-1}) vs. rates of dark respiration (μmol O_2 h^{-1} mg^{-1}) for *I. cuneata* ($R^2 = 0.0012$, P ns) and *P. cylindrica* ($R^2 = 0.2529$, $P < 0.001$). Individual relationships are only significant for *P. cylindrica* in the medium scenario ($R^2 = 0.6528$, $P < 0.001$). Microbioerosion (%) vs. relative abundance (%) of *Ostreobium* spp. ($n = 5$ tanks) for *I. cuneata* ($R^2 = 0.0696$, P ns) and *P. cylindrica* ($R^2 = 0.3869$, $P < 0.05$). Individual regressions were not significant.

understand how the boring abilities of endolithic species may be altered across the turbidity and/or bathymetric range.

By using combined pCO_2–temperature scenarios based on IPCC projections it was not possible to identify whether observed responses were the result of SW pCO_2, temperature, or whether their interaction is antagonistic or synergistic. A factorial design is clearly required to distinguish the role of each climate-related factor on the biological and physiological responses of endolithic algae. This, however, was not the aim of this study.

Conclusions

Our research demonstrated that endolithic microborers play a major role in mediating the dissolution of coral skeletons under projected ocean acidification and warming scenarios. The enhanced dissolution of coral skeletons by photosynthetic microborers under elevated pCO_2–temperature conditions is likely to be more variable than previously predicted, as particular coral skeletons differentially responded to the future scenarios. Nevertheless, the impact of microborers will be

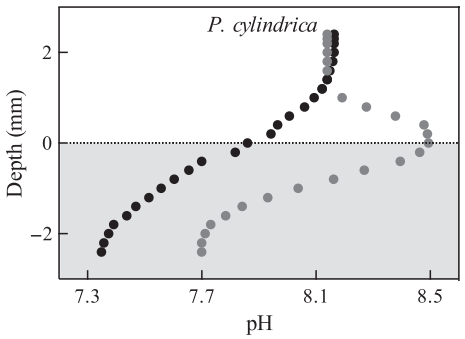

Fig. 5 Depth profiles of pH (steps of 200 μm) within the skeleton of *P. cylindrica* measured under dark (0 μmol quanta m^{-2} s^{-1} = black circles) and light conditions (900 quanta m^{-2} s^{-1} = gray circles) in the control pCO_2–temperature scenario (n = 1). Experimental flow rate was ca. 0.02 l s^{-1}. The horizontal dotted line marks the skeleton surface (0 mm depth), the gray area corresponds to measurements within the skeleton (from 0 to −2.4 mm) and the white represents the bulk seawater (from 0 to 2.4 mm).

greater for 'business as usual', than for 'reduced' pCO_2 emission scenarios for the temporal period in which the experiment was performed. Conditions within projected future oceans appeared to influence the biological and ecological responses of endolithic microborers resulting in increased dissolution of coral skeletons. This was demonstrated by the enhanced biomass, shifts in community structure, and increased respiration rates of endolithic algae under elevated pCO_2–temperature treatments. Together, our results provide insights into the processes and potential drivers regulating dissolution and the contribution of coral skeletal microbioerosion to net carbonate losses under projected ocean acidification and warming scenarios.

Acknowledgments

We thank G. Morelli for help during the experiment period; the staff at Heron Island Research Station for their technical assistance in the field; and T. Miard and A. Chai for maintaining the pCO_2–temperature system. We specially thank A. Rodriguez-Ramirez for help during field and laboratory work, constructive discussions, and valuable comments on this manuscript. The research reported here was funded by ARC CE0561435, ARC LP110200674, ARC LP0989845, Queensland Smart State Premier's Fellowship, and the Great Barrier Reef Foundation (GBRF). Samples collection was conducted under GBRMPA permit number G11/34255.1

References

Anderson MJ, Gorley RN, Clarke KR (2008) *PERMANOVA+ for PRIMER: guide to Software and Statistical Methods*, PRIMER-E Ltd., Plymouth, UK.

Andersson AJ, Gledhill D (2012) Ocean acidification and coral reefs: effects on breakdown, dissolution, and net ecosystem calcification. *Annual Review of Marine Science*, **5**, 1.1–1.28.

Andersson A, Bates N, Mackenzie F (2007) Dissolution of carbonate sediments under rising pCO_2 and ocean acidification: observations from Devil's Hole, Bermuda. *Aquatic Geochemistry*, **13**, 237–264.

Andersson AJ, Mackenzie FT, Bates NR (2008) Life on the margin: implications of ocean acidification on Mg-calcite, high latitude and cold-water marine calcifiers. *Marine Ecology Progress Series*, **373**, 265–273.

Andersson AJ, Kuffner IB, Mackenzie FT, Jokiel PL, Rodgers KS, Tan A (2009) Net loss of $CaCO_3$ from a subtropical calcifying community due to seawater acidification: mesocosm-scale experimental evidence. *Biogeosciences*, **6**, 1811–1823.

Anthony KRN, Kline DI, Diaz-Pulido G, Dove S, Hoegh-Guldberg O (2008) Ocean acidification causes bleaching and productivity loss in coral reef builders. *Proceedings of the National Academy of Sciences*, **105**, 17442–17446.

Atkinson MJ, Cuet P (2008) Possible effects of ocean acidification on coral reef biogeochemistry: topics for research. *Marine Ecology Progress Series*, **373**, 249–256.

Baird AH, Marshall PA (2002) Mortality, growth and reproduction in scleractinian corals following bleaching on the Great Barrier Reef. *Marine Ecology Progress Series*, **237**, 133–141.

Caldeira K, Wickett ME (2003) Anthropogenic carbon and ocean pH. *Nature*, **425**, 365.

Chazottes V, Le Campion-Alsumard T, Peyrot-Clausade M, Cuet P (2002) The effects of eutrophication-related alterations to coral reef communities on agents and rates of bioerosion (Reunion Island, Indian Ocean). *Coral Reefs*, **21**, 375–390.

Chazottes V, Cabioch G, Golubic S, Radtke G (2009) Bathymetric zonation of modern microborers in dead coral substrates from New Caledonia-Implications for paleodepth reconstructions in Holocene corals. *Palaeogeography, Palaeoclimatology, Palaeoecology*, **280**, 456–468.

Clarke KR (1993) Non-parametric multivariate analyses of changes in community structure. *Australian Journal of Ecology*, **18**, 117–143.

Crawley A, Kline DI, Dunn S, Anthony K, Dove S (2010) The effect of ocean acidification on symbiont photorespiration and productivity in Acropora formosa. *Global Change Biology*, **16**, 851–863.

Cuif JP, Dauphin Y, Gautret P (1999) Compositional diversity of soluble mineralizing matrices in some resent coral skeletons compared to fine-scale growth structures of fibres: discussion of consequences for biomineralization and diagenesis. *International Journal of Earth Sciences*, **88**, 582–592.

Cuif JP, Dauphin Y, Berthet P, Jegoudez J (2004) Associated water and organic compounds in coral skeletons: quantitative thermogravimetry coupled to infrared absorption spectrometry. *Geochemistry Geophysics Geosystems*, **5**, 1–9.

Davies SP (1989) Short-term growth measurements of corals using an accurate buoyant weighing technique. *Marine Biology*, **101**, 389–395.

Diaz-Pulido G, Mccook LJ (2002) The fate of bleached corals: patterns and dynamics of algal recruitment. *Marine Ecology Progress Series*, **232**, 115–128.

Diaz-Pulido G, Anthony KRN, Kline DI, Dove S, Hoegh-Guldberg O (2012) Interactions between ocean acidification and warming on the mortality and dissolution of coralline algae. *Journal of Phycology*, **48**, 32–39.

Dickson AG, Millero FJ (1987) A comparison of the equilibrium constants for the dissociation of carbonic acid in seawater media. Deep-Sea Research Part A. *Oceanographic Research Papers*, **34**, 1733–1743.

Dickson AG, Afghan JD, Anderson GC (2003) Reference materials for oceanic CO_2 analysis: a method for the certification of total alkalinity. *Marine Chemistry*, **80**, 185–197.

Dupraz C, Reid RP, Braissant O, Decho AW, Norman RS, Visscher PT (2009) Processes of carbonate precipitation in modern microbial mats. *Earth-Science Reviews*, **96**, 141–162.

Fine M, Loya Y (2002) Endolithic algae: an alternative source of photoassimilates during coral bleaching. Proceedings of the Royal Society of London. *Series B: Biological Sciences*, **269**, 1205–1210.

Fine M, Meroz-Fine E, Hoegh-Guldberg O (2005) Tolerance of endolithic algae to elevated temperature and light in the coral Montipora monasteriata from the southern Great Barrier Reef. *Journal of Experimental Biology*, **208**, 75–81.

Försterra F, Häeussermann V (2008) Unusual symbiotic relationships between microendolithic phototrophic organisms and azooxanthellate cold-water corals from Chilean fjords. *Marine Ecology Progress Series*, **370**, 121–125.

Garcia-Pichel F (2006) Plausible mechanisms for the boring on carbonates by microbial phototrophs. *Sedimentary Geology*, **185**, 205–213.

Garcia-Pichel F, Ramirez-Reinat E, Gao Q (2010) Microbial excavation of solid carbonates powered by P-type ATPase-mediated transcellular Ca^{2+} transport. *Proceedings of the National Academy of Sciences of the United States of America*, **107**, 21749–21754.

Golubic S, Perkins R, Lukas K, Frey R(1975) Boring microorganisms and microborings in carbonate substrates. In: *The Study of Trace Fossils: a Synthesis of Principles, Problems, and Procedures in Ichnology*. (ed Frey RW) pp 229. Springer-Verlag, New York.

Golubic S, Friedmann I, Schneider J (1981) The lithobiontic ecological niche, with special reference to microorganisms. *Journal of Sedimentary Petrology*, **51**, 475–478.

Gutner-Hoch E, Fine M (2011) Genotypic diversity and distribution of Ostreobium quekettii within scleractinian corals. *Coral Reefs*, **30**, 643–650.

Heiri O, Lotter AF, Lemcke G (2001) Loss on ignition as a method for estimating organic and carbonate content in sediments: reproducibility and comparability of results. *Journal of Paleolimnology*, **25**, 101–110.

Hoegh-Guldberg O, Fine M, Skirving W, Ron J, Dove S, Strong A (2005) Coral bleaching following wintry weather. *Limnology and Oceanography*, **50**, 265–271.

Hoegh-Guldberg O, Mumby PJ, Hooten AJ *et al.* (2007) Coral reefs under rapid climate change and ocean acidification. *Science*, **318**, 1737–1742.

Holmes G (2008) Estimating three-dimensional surface areas on coral reefs. *Journal of Experimental Marine Biology and Ecology*, **365**, 67–73.

Hughes TP, Baird AH, Bellwood DR *et al.* (2003) Climate change, human impacts, and the resilience of coral reefs. *Science*, **301**, 929–933.

Humm HJ, Wicks SR (1980) *Introduction and Guide to Marine Bluegreen Algae*, John Wiley & Sons, Inc. New York.

Ipcc (2007) *Climate Change 2007: synthesis Report. Contribution of Working Groups I, II and III to the Fourth Assessment Report of the Intergovernmental Panel on Climate Change*, IPCC, Geneva.

Jokiel P, Rodgers K, Kuffner I, Andersson A, Cox E, Mackenzie F (2008) Ocean acidification and calcifying reef organisms: a mesocosm investigation. *Coral Reefs*, **27**, 473–483.

Kiene W, Radtke G, Gektidis M, Golubic S, Vogel K (1995) Factors controlling the distribution of microborers in Bahamian reef environments. *Facies*, **32**, 176–188.

Kleypas J, Buddemeier R, Gattuso J-P (2001) The future of coral reefs in an age of global change. *International Journal of Earth Sciences*, **90**, 426–437.

Kleypas JA, Feely RA, Fabry VJ, Langdon C, Sabine CL, Robbins LL (2006) *Impacts of ocean ccidification on coral reefs and other marine calcifiers: a guide for future research*, NSF, NOAA, and the U.S. Geological Survey, St. Petersburg FL.

Kleypas JA, Danabasoglu G, Lough JM (2008) Potential role of the ocean thermostat in determining regional differences in coral reef bleaching events. *Geophysical Research Letters*, **35**, L03613.

Langdon C, Atkinson MJ(2005) Effect of elevated pCO_2 on photosynthesis and calcification of corals and interactions with seasonal change in temperature/irradiance and nutrient enrichment. *Journal of Geophysical Research*, **110**, C09S07.

Le Campion-Alsumard T, Golubic S, Hutchings P (1995) Microbial endoliths in skeletons of live and dead dead corals: porites lobata (Moorea, French-Polynesia). *Marine Ecology Progress Series*, **117**, 149–157.

Lukas KJ (1974) Two species of chlorophyte genus Ostreobium from skeletons of Atlantic and Caribbean reef corals. *Journal of Phycology*, **10**, 331–335.

Magnusson SH, Fine M, Kuhl M (2007) Light microclimate of endolithic phototrophs in the scleractinian corals Montipora monasteriata and Porites cylindrica. *Marine Ecology Progress Series*, **332**, 119–128.

Manzello DP, Kleypas JA, Budd DA, Eakin CM, Glynn PW, Langdon C (2008) Poorly cemented coral reefs of the eastern tropical Pacific: possible insights into reef development in a high-CO_2 world. *Proceedings of the National Academy of Sciences*, **105**, 10450–10455.

Martin S, Gattuso J-P (2009) Response of Mediterranean coralline algae to ocean acidification and elevated temperature. *Global Change Biology*, **15**, 2089–2100.

Meehl GA, Stocker TF, Collins WD *et al.* (2007) Global Climate Projections. In: *Climate Change 2007: the Physical Science Basis. Contribution of Working Group I To The Fourth Assessment Report of the Intergovernmental Panel On Climate Change*. (eds Solomon S, Qin D, Manning M, Chen Z, Marquis M, Averyt KB, Tignor M, Miller HL) pp 747–845. Cambridge University Press, Cambridge.

Mehrbach C, Culberso CH, Hawley JE, Pytkowic RM (1973) Measurement of apparent dissociation-constants of carbonic-acid in seawater at atmospheric pressure. *Limnology and Oceanography*, **18**, 897–907.

Nagarkar S (1998) New records of marine cyanobateria from rocky shores of Hong Kong. *Botanica Marina*, **41**, 527–542.

Nothdurft LD, Webb GE, Bostrom T, Rintoul L (2007) Calcite-filled borings in the most recently deposited skeleton in live-collected Porites (Scleractinia): implications for trace element archives. *Geochimica Et Cosmochimica Acta*, **71**, 5423–5438.

Orr JC, Fabry VJ, Aumont O *et al.* (2005) Anthropogenic ocean acidification over the twenty-first century and its impact on calcifying organisms. *Nature*, **437**, 681–686.

Perry CT (1998) Grain susceptibility to the effects of microboring: implications for the preservation of skeletal carbonates. *Sedimentology*, **45**, 39–51.

Pierrot D, Lewis E, Wallace D (2006) *MS Excel Program Developed For CO_2 System Calculations*. Carbon Dioxide Information Analysis Center Oak Ridge National Laboratory, U.S Department of Energy, Oak Ridge, Tennessee.

Ramirez-Reinat EL, Garcia-Pichel F (2012) Prevalence of Ca^{2+}-ATPase-mediated carbonate dissolution among cyanobacterial euendoliths. *Applied and Environmental Microbiology*, **78**, 7–13.

Reyes-Nivia MC, Garzon-Ferreira J, Rodriguez-Ramirez A (2004) Live coral predation by fish in Tayrona Natural National Park, Colombian Caribbean. *Revista de Biología Tropical*, **52**, 883–895.

Riding R (2000) Microbial carbonates: the geological record of calcified bacterial–algal mats and biofilms. *Sedimentology*, **47**, 179–214.

Sokal RR, Rohlf F (1995) *Biometry*. WH Freemand and Company, New York.

Tribollet A (2008a) The boring microflora in modern coral reef ecosystems: a review of its roles. In: *Current Developments in Bioerosion* (eds Wisshak M, Tapanila L), pp. 67–94. Springer-Verlag Berlin Heidelberg, Berlin.

Tribollet A (2008b) Dissolution of dead corals by euendolithic microorganisms across the Northern Great Barrier Reef (Australia). *Microbial Ecology*, **55**, 569–580.

Tribollet A, Godinot C, Atkinson M, Langdon C(2009) Effects of elevated pCO_2 on dissolution of coral carbonates by microbial euendoliths. *Global Biogeochemical Cycles*, **23**, GB3008.

Underwood AJ (1997) *Experiments In Ecology: their Logical Design And Interpretation Using Analysis Of Variance*. Cambridge University Press, New York.

Vogel K, Gektidis M, Golubic S, Kiene WE, Radtke G (2000) Experimental studies on microbial bioerosion at Lee Stocking Island, Bahamas and One Tree Island, Great Barrier Reef, Australia: implications for paleoecological reconstructions. *Lethaia*, **33**, 190–204.

Walter LM, Bischof SA, Patterson WP *et al.* (1993) Dissolution and recrystallization in modern shelf carbonates: evidence from pore water and solid phase chemistry. Philosophical Transactions of the Royal Society of London. *Series A: Physical and Engineering Sciences*, **344**, 27–36.

Wisshak M, Schönberg CHL, Form A, Freiwald A (2012) Ocean acidification accelerates reef bioerosion. *PLoS ONE*, **7**, e45124.

Supporting Information

Additional Supporting Information may be found in the online version of this article:

Fig. S1. (a) Endolithic algae inhabiting live *Isopora cuneata* and (b) *Porites cylindrica*. Arrows pointing the location of green bands of endolithic algae. (c) After careful cleaning of epilithic algae to perform respirometry assays and biomass estimations.